ORIGINAL ARTICLE

Finite element method for solving geodetic boundary value problems

Zuzana Fašková · Róbert Čunderlík · Karol Mikula

Abstract The goal of this paper is to present the finite element scheme for solving the Earth potential problems in 3D domains above the Earth surface. To that goal we formulate the boundary-value problem (BVP) consisting of the Laplace equation outside the Earth accompanied by the Neumann as well as the Dirichlet boundary conditions (BC). The 3D computational domain consists of the bottom boundary in the form of a spherical approximation or real triangulation of the Earth's surface on which surface gravity disturbances are given. We introduce additional upper (spherical) and side (planar and conical) boundaries where the Dirichlet BC is given. Solution of such elliptic BVP is understood in a weak sense, it always exists and is unique and can be efficiently found by the finite element method (FEM). We briefly present derivation of FEM for such type of problems including main discretization ideas. This method leads to a solution of the sparse symmetric linear systems which give the Earth's potential solution in every discrete node of the 3D computational domain. In this point our method differs from other numerical approaches, e.g. boundary element method (BEM) where the potential is sought on a hypersurface only. We apply and test FEM in various situations. First, we compare the FEM solution with the known exact solution in case of homogeneous sphere. Then, we solve the geodetic BVP in continental scale using the DNSC08 data. We compare the results with the EGM2008 geopotential model. Finally, we study the precision of our solution by the GPS/levelling test in Slovakia where we use terrestrial gravimetric measurements as input data. All tests show qualitative and quantitative agreement with the given solutions.

1 Introduction

Nowadays, an importance and efficiency of numerical methods have rapidly increased with the development of high-performance computing (HPC) facilities. With numerical methods we are able to get numerical solutions of physical problems described by partial differential equations (PDE) in complicated 3D geometries. A solution of the external geodetic boundary-value problem (BVP) is an important theoretical and practical issue in geodesy and needs indepth tools and methods of applied mathematics. At present, the global gravity field modelling is mainly performed by spherical harmonics and precise local modelling by the FFT-based methods (e.g. Sideris and Schwarz 1986) and the geodetic collocation (e.g. Tscherning 1978). From numerical methods, the boundary element method (BEM) has been recently used by various groups to determine Earth's gravity field (e.g. Klees 1992, 1995, 1998; Klees et al. 2001; Lehmann 1977, 1997; Čunderlík et al. 2000; Čunderlík 2004; Čunderlík et al. 2008). The variational method based on a weak formulation and minimization of a function was developed in Holota and Nesvadba (2008) and Nesvadba et al. (2007). In case of the finite element method (FEM), the pioneering work has been done by Meissl (1981) and

Z. Fašková (✉) · R. Čunderlík · K. Mikula
Faculty of Civil Engineering, Slovak University of Technology,
Radlinského 11, 813 68 Bratislava, Slovakia
e-mail: faskova@math.sk; zuzana.faskova@stuba.sk

R. Čunderlík
e-mail: cunderli@svf.stuba.sk

K. Mikula
e-mail: mikula@math.sk

Shaofeng and Dingbo (1991). The goal of this paper is to present the finite element technique for the solution of the Earth potential problems related to physical geodesy in 3D domains.

At present, thanks to the precise 3D positioning by GNSS that accompanies gravimetric measurements, more attention has been focused on the fixed gravimetric BVP. Here, the physical surface of the Earth is assumed to be known. A uniqueness theorem for a non-linear fixed gravimetric BVP was first given by Backus (1968). The existence and uniqueness of the solution for the associated linear problem were introduced by Koch and Pope (1972). They also gave a uniqueness proof for the non-linear case. This general problem was later discussed by Bjerhammar and Svensson (1983), Sacerdote and Sansó (1989) and Grafarend (1989). Later, many authors have dealt with the fixed gravimetric BVP (e.g. Holota 1997, 2005).

In spite of previous approaches, where the solution is usually sought on a 2D hypersurface given by a sphere, ellipsoid or the Earth's surface, here we solve the geodetic BVP in 3D domains above the Earth surface. After discretization it leads to sparse linear systems which are comparable with full BEM matrices regarding the computational complexity and we get directly the Earth's potential solution in the whole 3D computational domain.

The FEM assumes the discretization of the domain by a set of subdomains—the finite elements. In order to derive the FEM model, a weak formulation of the differential equation on every element is constructed. Since any continuous function can be represented by a linear combination of the algebraic polynomials, a numerical solution is sought as a linear combination of nodal values and approximation functions. The balance of the interelement fluxes and continuity of the numerical solution on interelement boundaries are used to assemble the whole solution. Taking into account the boundary condition (BC), the global linear system of equations can be solved. For FEM analysis, we use the FEM software ANSYS with its 3D 4- and 8-node linear elements.

In order to obtain the numerical solution to the geodetic BVP by our approach using FEM, we provide the following particular tasks. The theoretical formulation of our geodetic BVP is given, the derivation of FEM model for this problem and some numerical experiments are described. First, in case of a potential generated by the homogeneous sphere, we compare our solution with the known exact solution to find out the experimental order of convergence (EOC). Then solving geodetic BVP in global and continental scale using DNSC08 gravity data, we compare the results with the EGM2008 (Pavlis et al. 2008) geopotential model. Finally, we use terrestrial gravimetric measurements as input data and test the precision of our obtained solution by the GPS/levelling in the area of Slovakia.
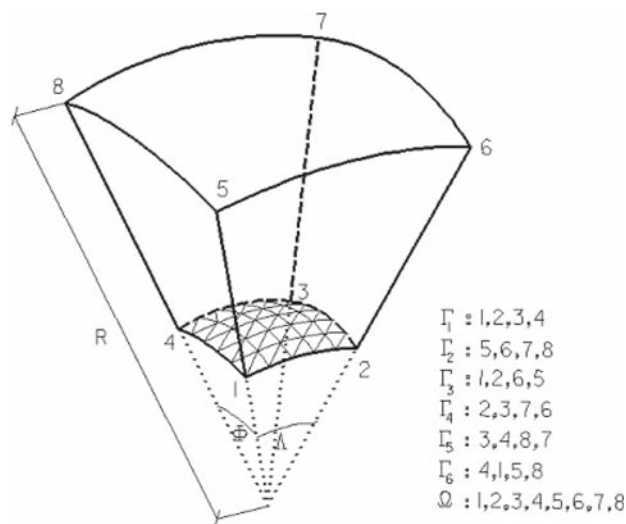
Fig. 1 Illustration of the computational domain, the Earth's surface Γ_1 is approximated by series of *triangles*

2 Formulation of the geodetic BVP

Let us consider the linearized fixed gravimetric BVP (cf. Koch and Pope 1972; Holota 1997, 2005; Čunderlík et al. 2008).

$$-\Delta T(\mathbf{x}) = 0, \quad \mathbf{x} \in R^3 - \Omega, \tag{1}$$

$$\langle \nabla T(\mathbf{x}), \bar{s}(\mathbf{x}) \rangle = -\delta g(\mathbf{x}), \quad \mathbf{x} \in \partial\Omega, \tag{2}$$

$$T(x) \to 0 \quad as \quad |x| \to \infty, \tag{3}$$

where $T(\mathbf{x})$ is the disturbing potential defined as a difference between the real $W(\mathbf{x})$ and normal $U(\mathbf{x})$ gravity potential at any point $\mathbf{x}$ under the assumptions discussed in Holota (1997), $\delta g(\mathbf{x})$ is the gravity disturbance and $\bar{s}(\mathbf{x}) = \nabla U(\mathbf{x})/|\nabla U(\mathbf{x})|$.

Although the BVP (1)–(3) deals with the infinite domain, in our approach using the FEM we construct an artificial boundary $\Gamma_2 \subset \partial\Omega$ away from the approximate Earth surface (Fig. 1), and due to the giant size of the Earth we restrict our computations only to a partial domain Ω depicted in Fig. 1 as well. The bottom surface $\Gamma_1 \subset \partial\Omega$ represents a part of the Earth surface, given by a sphere (in our global and local quasi-igeoidal solution) or discretized by triangles (regional quasi-igeoidal solution). The surface gravity disturbances in (2) represent the oblique derivative BC (neglecting the deflection of the vertical). In order to get the Neumann BC, we project the oblique derivative BC into the boundary Γ_1, i.e. $\frac{\partial T(\mathbf{x})}{\partial n_{\Gamma_1}}$ is approximately equal to $-\delta g(\mathbf{x}). \cos \mu(\mathbf{x})$, where $\mu(\mathbf{x})$ is the angle $\angle (\bar{s}(\mathbf{x}), n_{\Gamma_1}(\mathbf{x}))$. It is worth to note that this term represents the projection of the vector $\delta g(\mathbf{x})\bar{s}(\mathbf{x})$ (not exactly of the vector $\nabla T(\mathbf{x})$) to the normal n_{Γ_1}. In this way, the oblique derivative BC in (2) is incorporated into our FEM formulation similarly as it was used for BEM in Čunderlík et al. (2008). The upper spherical part $\Gamma_2 = \{x; |x| = R\}$ of the domain

represents the artificial boundary where the Dirichlet BC is prescribed. On the further side planar boundaries $\Gamma_{4,6} \subset \partial\Omega$ and side conical boundaries $\Gamma_{3,5} \subset \partial\Omega$, we use the Dirichlet BC. Then our geodetic BVP is defined as follows:

$$-\Delta T(\mathbf{x}) = 0, \quad \mathbf{x} \in \Omega, \tag{4}$$

$$\frac{\partial T(\mathbf{x})}{\partial n_{\Gamma_1}} = -\delta g^*(\mathbf{x}) = -\delta g(\mathbf{x}) \cdot \cos\mu(\mathbf{x}),$$

$$\mu(\mathbf{x}) = \angle\,(\bar{s}(\mathbf{x}), n_{\Gamma_1}^-(\mathbf{x})), \mathbf{x} \in \Gamma_1 \tag{5}$$

$$T(\mathbf{x}) = T_{\mathrm{SAT}}(\mathbf{x}), \mathbf{x} \in \Gamma_i, i = 2, \ldots, 6, \tag{6}$$

where T_{SAT} represents the disturbing potential generated from a satellite geopotential model. The problem (4)–(6) contains both the Neumann and Dirichlet BCs, so we call it the geodetic BVP with mixed BC.

3 Solution of the geodetic BVP by finite element method

To derive the variational formulation of (4)–(6), we define the Sobolev space of test functions V, i.e. the space of functions from $W_2^{(1)}(\Omega)$ which are equal to 0 on Γ_i, $i = 2, \ldots, 6$, in the sense of traces. We multiply the differential equation (4) by $v \in V$ and get

$$\int_\Omega \nabla T \cdot \nabla v \, \mathrm{d}x\mathrm{d}y\mathrm{d}z - \int_{\partial\Omega} \nabla T \cdot n \, v \, \mathrm{d}\sigma = 0, \quad \forall v \in V. \tag{7}$$

Let the extension of Dirichlet BC given by T_{SAT} into the domain Ω be in $W_2^{(1)}(\Omega)$ and let $\delta g^* \in L^2(\Gamma_1)$. Then we define the weak formulation of our BVP (4)–(6) as follows: we look for a function T, such that $T - T_{\mathrm{SAT}} \in V$ and

$$\int_\Omega \nabla T \cdot \nabla v \, \mathrm{d}x\mathrm{d}y\mathrm{d}z + \int_{\Gamma_1} \delta g^* v \, \mathrm{d}\sigma = 0, \quad \forall v \in V. \tag{8}$$

Due to Brenner and Scott (2002) or Rektorys (1974), the solution of this problem always exists and is unique. Moreover, the finite element approximation described below converges to the weak solution refining the finite element grid.

The FEM assumes discretization of the domain by a set of subdomains called the finite elements, cf. Figs. 2 and 3, and V_h, the finite dimensional subspace of V, corresponding to
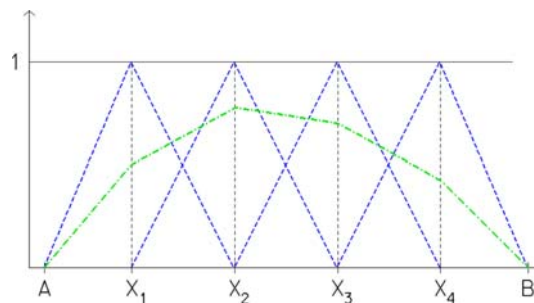
Fig. 2 Discretization of 1D domain, basis functions v_i (*blue dashed lines*) and their linear combination (*green dot-and-dash line*) that is piecewise linear

the finite element grid is chosen. In order to complete the discretization, we must select a basis of V_h. In 1D case (Fig. 2), for each nodal point x_i we will choose the piecewise linear function $v_i \in V$ whose value is equal to 1 at x_i and zero at every x_j, $i \neq j$, i.e.

$$v_i(x) = \begin{cases} \dfrac{x - x_{i-1}}{x_i - x_{i-1}} & \text{if } x \in [x_{i-1}, x_i], \\ \dfrac{x_{i+1} - x}{x_{i+1} - x_i} & \text{if } x \in [x_i, x_{i+1}], \\ 0 & \text{otherwise}, \end{cases}$$

for $i = 1, \ldots, n$. In the case of 2D and 3D computational domains, we follow the similar way, i.e. we choose again one basis function v_i per vertex x_i. The function v_i is uniquely determined by choosing value 1 at x_i and zero at every x_j, $i \neq j$. The plot of such basis functions for triangular and rectangular 2D finite element grids is given in Fig. 4.

The principal advantage of such piecewise linear basis is that the inner products

$$\langle v_i, v_j \rangle = \int_A^B v_i v_j \, \mathrm{d}x, \qquad \phi(v_i, v_j) = \int_A^B v_i' v_j' \, \mathrm{d}x \tag{9}$$

will be zero for all i, j when holds $|i - j| > 1$. In 1D case, the support of v_i is the interval $[x_{i-1}, x_{i+1}]$. Hence, the integrands of $\langle v_i, v_j \rangle$ and $\phi(v_i, v_j)$ are identically zero whenever $|i - j| > 1$. In the 2D and 3D cases likewise in 1D case, if x_i and x_j do not share a common edge of the discretization,

Fig. 3 Example of discretization of a planar domain by *triangular* and *rectangular* elements
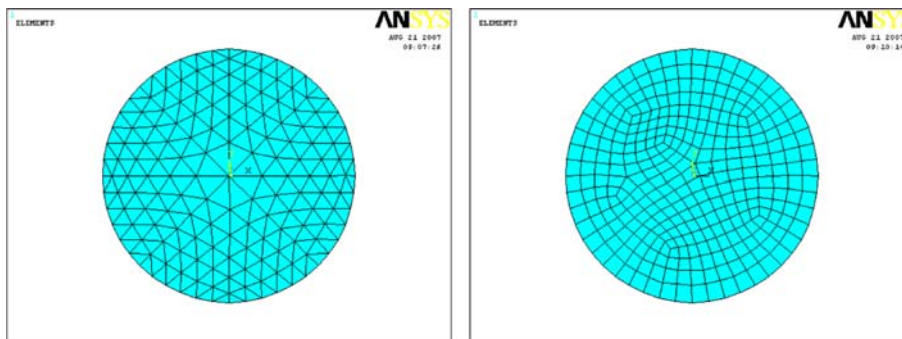
Fig. 4 Piecewise linear basis function on 2D domain discretized by *triangles* and bilinear basis function on 2D domain discretized by *squares*
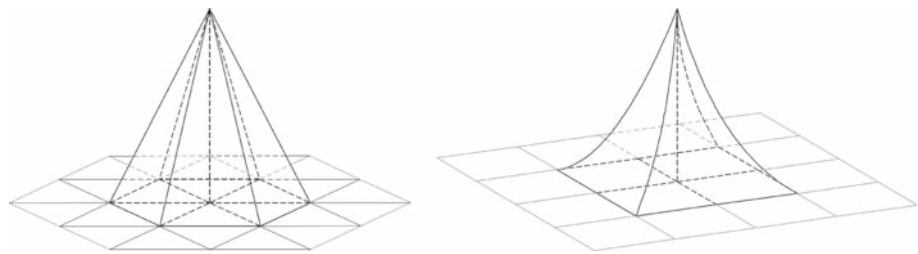
Table 1 Errors for the example of potential generated by unit sphere

Experiment	A		B		C	
E	$\|\mathbf{u} - u\|_{L_2(\Omega)}$	EOC	$\|\mathbf{u} - u\|_{L_2(\Omega)}$	EOC	$\|\mathbf{u} - u\|_{L_2(\Omega)}$	EOC
2^3	0.006750	–	0.021179	–	0.005511	–
4^3	0.001053	2.68	0.004562	2.21	0.001018	2.43
8^3	0.000187	2.49	0.000989	2.21	0.000180	2.42
16^3	0.000036	2.37	0.000228	2.11	0.000040	2.29

Table shows that method is $O(h^2)$—second order accurate in L_2-norm

the integrals

$$\langle v_i, v_j \rangle = \int_\Omega v_i v_j \; \mathrm{d}x\mathrm{d}y\mathrm{d}z, \quad \phi(v_i, v_j) = \int_\Omega \nabla v_i \cdot \nabla v_j \; \mathrm{d}x\mathrm{d}y\mathrm{d}z \tag{10}$$

are both zero.

If we write $T^n(x, y, z) = \sum_{j=1}^n t_j v_j(x, y, z)$, i.e. take an approximation of T as T^n, a linear combination of basis functions with coefficients t_i, $i = 1, \ldots, n$, plug it into the weak formulation (8) and consider test function $w = v_i$ we get

$$\sum_{j=1}^n t_j \phi(v_i, v_j) = q_i, \quad i = 1, \ldots, n. \tag{11}$$

where $q_i = -\int_{\Gamma_1} \delta g^* v_i \; \mathrm{d}\sigma$.

Then let the column vectors $(t_1, \ldots, t_n)$ and $(q_1, \ldots, q_n)$ be denoted by $\mathbf{t}$ and $\mathbf{q}$, respectively, and let $K = [K_{ij}]$ be matrix whose entries are $K_{ij} = \phi(v_i, v_j)$. We may rephrase (11) as

$$K\mathbf{t} = \mathbf{q}, \tag{12}$$

which represents the linear system of equations for unknown nodal solution values $\mathbf{t}$. The matrix K is usually referred to as the stiffness matrix which is sparse since most of its entries are zero and, in addition, the matrix is symmetric and positive definite.

3.1 Numerical experiments by FEM

In the following section we present various numerical experiments performed by the FEM implemented in the ANSYS software.[1] The first experiment is theoretical to illustrate the order of accuracy of FEM. We suppose potential $u(\Lambda, \Phi, R)$

is generated by a homogeneous sphere with radius $R = 1$ m. We solve this problem in a space between $R = 1$ and 2 m. Since we know the exact solution, $u(\Lambda, \Phi, R) = 1/R$, we can easily compute the Dirichlet and Neumann BC. There is the Neumann BC on the bottom boundary applied in all experiments. In Experiment A, on upper spherical and on side boundaries the Dirichlet BC is considered. In experiment B, on the vertical boundaries the zero Neumann (reflective) BC, and on the upper spherical boundary the Dirichlet BC are applied. In the last theoretical experiment denoted by capital C on the upper spherical boundary the Neumann and on the side boundaries the Dirichlet BC are considered.

Now let us assume that the error of the scheme in some norm is proportional to some power of the grid size, i.e. $\mathrm{Error}(h) = Ch^\alpha$, with a constant C. Then halving the grid size we have $\mathrm{Error}(h/2) = C(h/2)^\alpha$ from where we can simply extract $\alpha = \log_2(\mathrm{Error}(h)/\mathrm{Error}(h/2))$. The α is called the EOC and can be determined by comparing numerical solutions and exact solutions on subsequently refined grids. One can see that FEM is second order accurate in all theoretical experiments (Table 1).

The following numerical experiments deal with the global gravity field modelling. We have performed computations in the western and eastern hemispheres with coarse grids—3D 8-node elements $2° \times 2°$ and $1° \times 1°$ based. As the input BC we use the DNSC08 gravity anomaly dataset. According to the authors Andersen et al. (2008), DNSC08_GRAV includes the altimetry-derived free-air gravity anomalies at oceans/seas augmented by EGM2008 on lands. Thus, for our purposes we interpolate the free-air gravity anomalies in the nodes on the bottom boundary Γ_1 from DNSC08_GRAV and transform them into the surface gravity disturbances using EGM2008. As the Dirichlet BC on Γ_i, $i = 2, \ldots, 6$ we use the disturbing potential generated from the ITG-GRACE03S satellite geopotential model (Mayer-Grr 2007) up to degree 180.

---

[1] ANSYS, online tutorial: www.ansys.com.

Fig. 5 Meshed subdomain and the input gravity disturbances
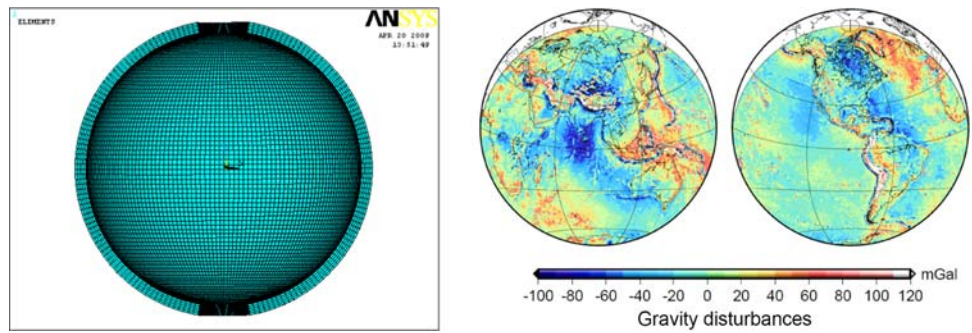
Fig. 6 Disturbing potential solution in eastern Ω_1 and western Ω_2 hemisphere
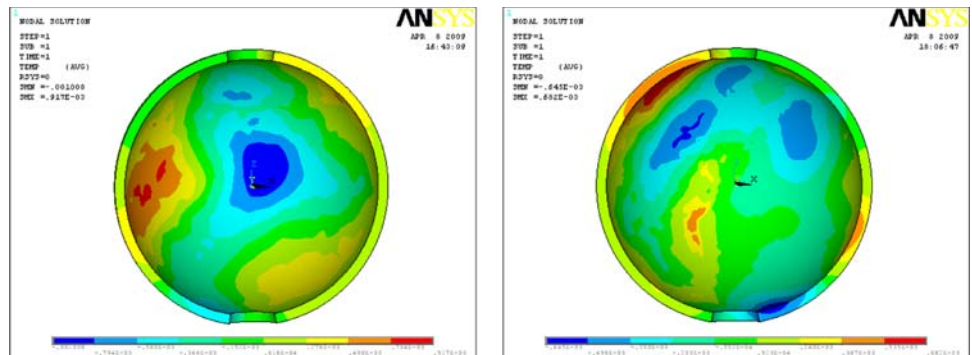
Table 2 Statistics of the residuals between the global FEM solutions and EGM2008

Hemisphere	Eastern	Western	Eastern	Western
Resolution (°)	2×2	2×2	1×1	1×1
No. of all nodes	44,226	44,226	174,846	174,846
No. of elements	36,000	36,000	144,000	144,000
Min. residual (m)	−15.92	−20.16	−9.70	−12.17
Mean residual (m)	0.22	−0.12	0.11	−0.05
Max. residual (m)	20.52	16.60	14.00	7.14
St. dev. (m)	2.20	1.89	1.10	0.93

Table 3 Geometry of computational domains representing different parts of the world and mesh statistics

	Europe	North America	South America	Indonesia
Resolution (°)	0.2×0.2	0.25×0.25	0.25×0.25	0.25×0.25
No. of all nodes	693,011	620,816	620,816	638,891
No. of elements	625,000	576,000	576,000	576,000
Sp. latitude	20, 70	20, 60	−50, 10	−30, 30
Sp. longitude	0, 50	230, 290	270, 330	120, 180

We consider the space above the sphere of radius $R_1 = 6,371$ km, where the Neumann BC (5) is given, up to the sphere with radius $R_2 = 6,871$ km, where the Dirichlet BC (6) is considered. Then the computations were performed in two subdomains Ω_1 and Ω_2, where $\Omega_1 : \Phi \times \Lambda_1 = (-80, 80) \times (0, 180)°$ and $\Omega_2 : \Phi \times \Lambda_2 = (-80, 80) \times (180, 360)°$, Φ is spherical latitude and Λ is spherical longitude. Afterwards each subdomain has been meshed with 8-node elements, creating five layers (Fig. 5). The FEM output (Fig. 6), being in the form of the disturbing potential as a nodal solution, has been transformed into the quasigeoidal heights above the ellipsoid. We have compared this solution with EGM2008 (Table 2).

The comparison shows that the refinement of the discretization improves a precision of the FEM solution. Namely, halving the element's side leads to decreasing of the standard deviation of the residuals by factor 2. One can see that the

mean values, which are in cm, tend to zero, in spite of the fact that the FEM solution is fixed to ITG-GRACE03S satellite geopotential model on the upper and side boundaries. We suppose that the further successive refinement would improve the precision of the FEM solution. However, it yields to large memory requirements. Therefore, in the following section, we restrict our quasigeoidal modelling to smaller areas of the continental scale.

3.2 Local quasigeoidal modelling

The computational domain is the space between two spheres, $R_1 = 6,371$ km and $R_2 = 6,871$ km, and spherical coordinates are dependent on the concrete location of computational domain (Table 3). Afterwards such domains are meshed with 8-node elements with base $0.25° \times 0.25°$ except of Europe where $0.2° \times 0.2°$-based elements were used. There

Table 4 Statistics of residuals between the local quasigeoidal solutions and EGM2008 in different parts of the world

|	Europe	North America	South America	Indonesia
No. of nodes on Γ_1	63,001	38,801	38,001	58,081
Min. residual	−2.056	−2.123	−4.000	−3.648
Mean residual	−0.027	0.020	0.033	0.032
Max. residual	1.496	1.612	5.327	2.888
St. dev.	0.175	0.194	0.355	0.293

are formed about 15 layers in R-direction. The FEM solution is compared with quasigeoidal heights generated from EGM2008 (Table 4). Figure 7 depicts the profiles across the FEM solution, EGM2008 and ITG-GRACE03S in the area of Europe to illustrate an influence of the prescribed Dirichlet BC on the FEM solution. It is evident from the profiles

depicted in Fig. 7 that a striping effect as well as eventual bias of the satellite geopotential model affects the FEM solution only in very close zones to the side boundaries. They have practically no impact on the central zones.

3.3 Regional quasigeoidal model

For our regional experiments we have chosen the space above Slovak Republic. As input data on the bottom boundary we have used the surface gravity disturbances obtained from the original terrestrial gravity measurements (Klobušiak and Pecár 2004) (Fig. 8). The Dirichlet BC on the upper and side boundaries are generated from EGM2008 up to degree 2,160. The real Earth's surface topography has been approximated by series of triangles sized 10, 8, 7 and 5 km. The upper boundary has been placed 150 or 200 km above the Earth's surface. The results have been tested at 61 GPS/levelling

Fig. 7 Profiles across the quasigeoidal models in Europe that show an influence of the Dirichlet BC on the side boundaries on the FEM solution
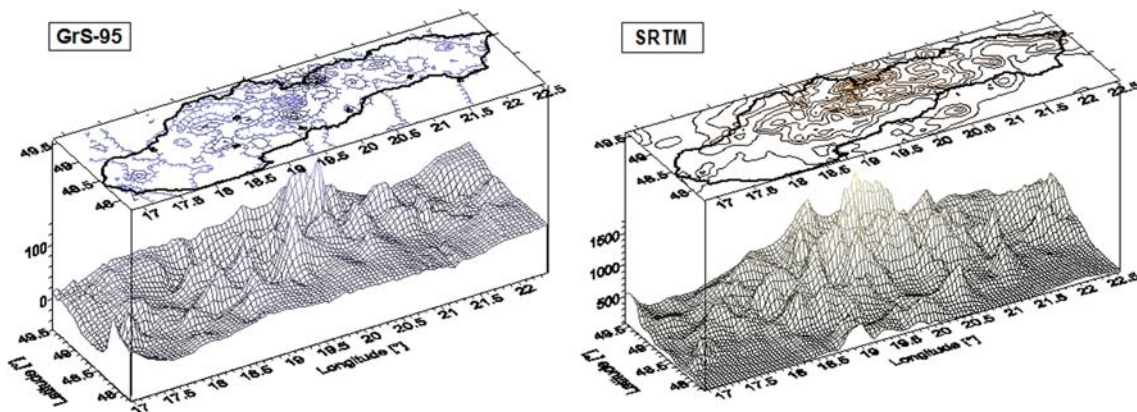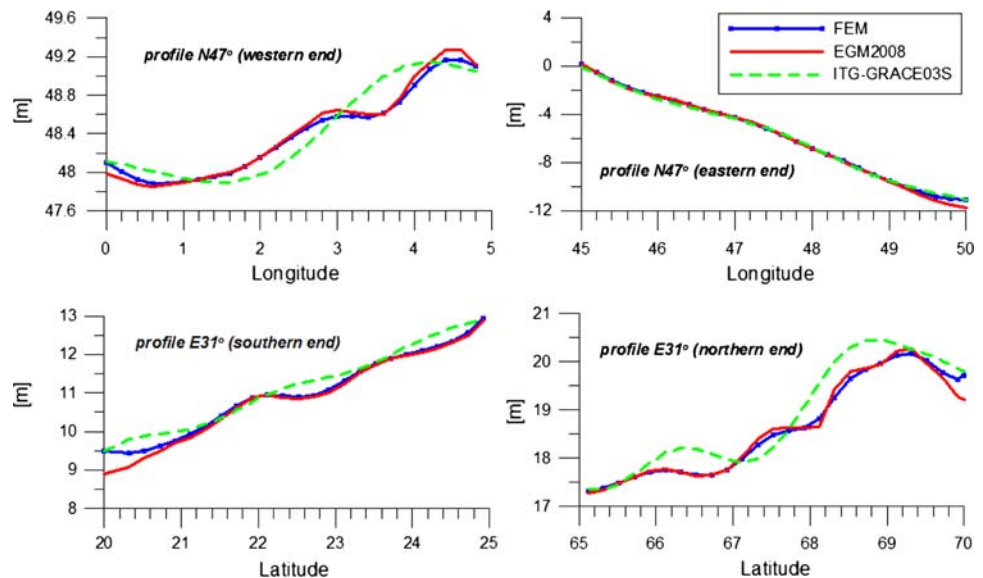
Fig. 8 Surface gravity disturbances computed from detailed gravimetric mapping GrS-95 and the terrain topography in Slovakia

Table 5 GPS/levelling test at 61 points for the regional quasigeoidal solutions by FEM with different sizes of approximating triangles, height of upper boundary: 150 km

| Element size	10 km	8 km	7 km	5 km
Min. residual	−0.424	−0.394	−0.388	−0.394
Mean residual	−0.221	−0.211	−0.223	−0.248
Max. residual	0.051	0.064	−0.022	−0.044
St. deviation	0.100	0.102	0.088	0.078
St. dev. after fitting	0.074	0.068	0.060	0.059

All characteristics are in meter

points. For the fitting process we have chosen the surface polynomial regression using the second degree polynomial surface with 6 coefficients (Mojzeš et al. 2006). The residuals after the fitting are depicted in Fig. 11 and statistics of the residuals are presented in Table 5. The next regional experiment treats an influence of the upper boundary. We have chosen the 5 km triangulation and made the computation with the height of the upper boundary: 250, 200, 150 and 100 km. Then we have computed the residuals between the GPS/levelling method and our solutions (the first two rows of Fig. 10). The difference between solutions 250 and 100 km are depicted in the last row of Fig. 10. One can see a pushing of the detailed character of real data down by the data on upper spherical boundary which is ineligible con-

sequence of lowering the upper boundary. According to the GPS/levelling tests for all regional experiments, we summarize:

– refinements of the discretization improve the FEM solution (Fig. 9 and Table 5),
– standard deviation of the residuals at GPS/levelling points for the most detailed quasigeoids model (resolution 5 km) using original gravity data is 7.8 and 5.9 cm after second-order polynomial fitting (Fig. 9 and Table 5). Such precision is a little bit worse than the quasigeoidal model obtained by the FFT-based methods (7.8 and 3.9 cm after fitting (Mojzeš et al. 2006)) but slightly better than the BEM solution (17.1 and 6.0 cm after fitting (Čunderlík et al. 2008)),
– the lowering of the upper spherical boundary with the input BC from geopotential models pushes the FEM solution especially local maxima in mountainous regions (Fig. 10) and
– the influence of the Dirichlet BC on the solution is not significant when the side boundaries are far enough (several elements).

Finally, we mention the following advantages of the proposed approach for the regional as well as global quasigeoidal modelling.


Fig. 9 Final quasigeoid models in the area of Slovak Republic for the different discretization levels and differences between them. Height of upper boundary: 150 km
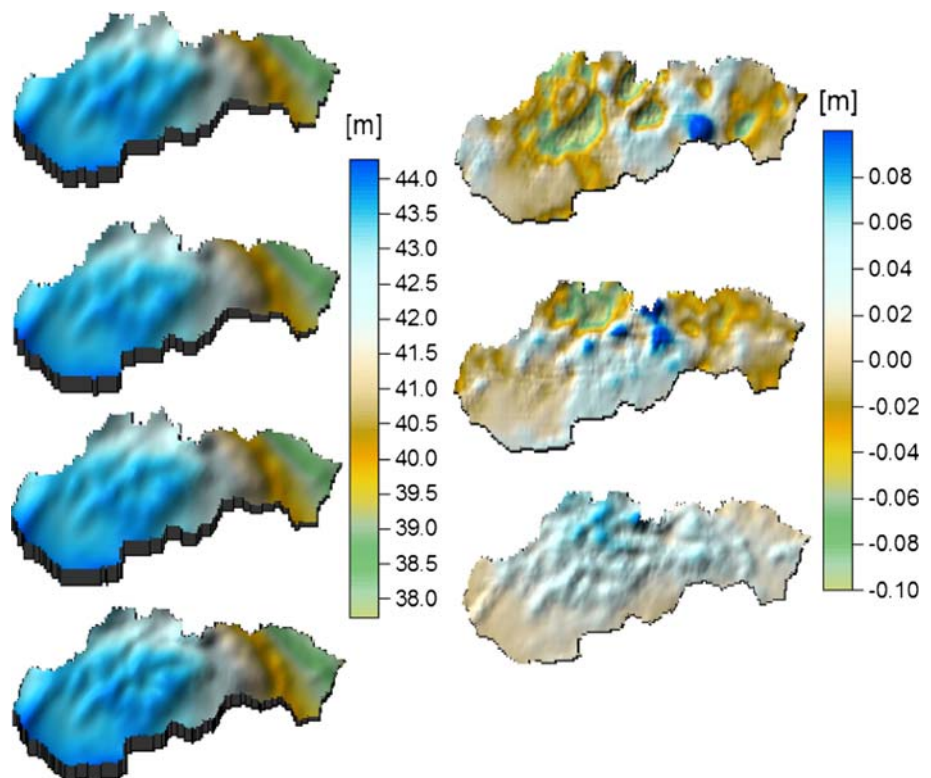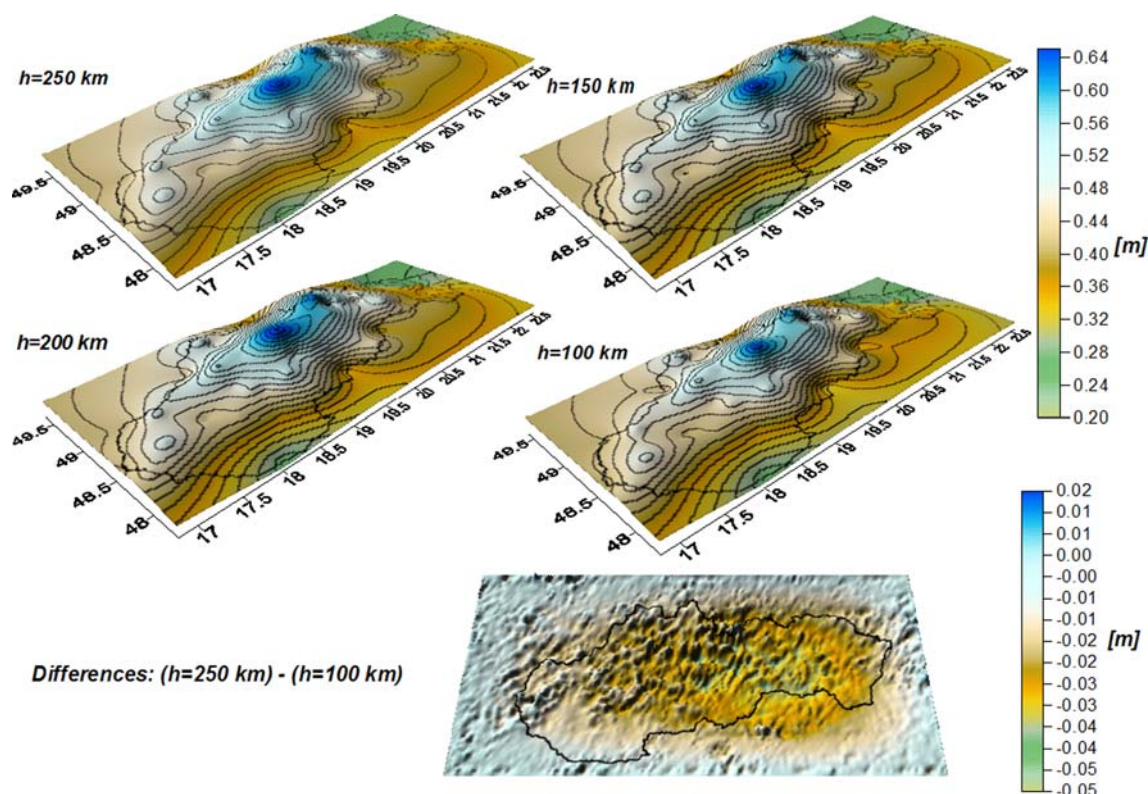
Fig. 10 Differences between the FEM solutions and the GPS/levelling method with 5 km discretization and the height of the upper boundary: 100, 150, 200 and 250 km

Fig. 11 GPS/levelling test residuals after second degree polynomial fitting
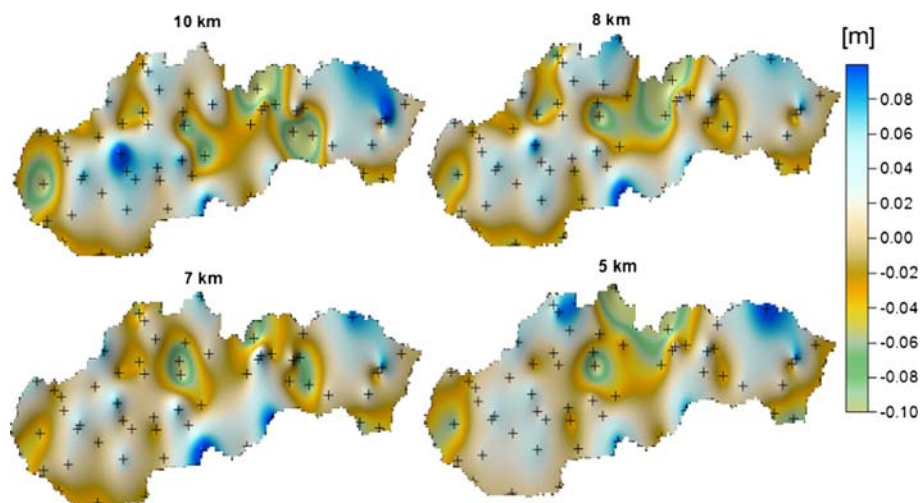
– It is not necessary to integrate over the whole Earth's surface only over the domain above the area of interest.
– The Dirichlet BC from satellite geopotential models fix the FEM solution but their eventual bias and striping effect do not influence the FEM solution in the central zones.
– The airborne gravimetric data can be applied as the Neumann BC on the upper boundary.

– Triangulation of the Earth's surface can be given from discrete terrestrial gravimetric measurements.
– Local refinement procedures can be applied in areas of interest.
– The further refinement of the discretization is straightforward that can be useful for the global gravity field modelling especially to model dynamical processes in the gravity field.

4 Conclusions

The main goal of this paper was to build the FEM which looks for the numerical solution in 3D domains above the Earth's surface. So we had to formulate the geodetic BVP in the 3D domain and we considered the Neumann as well as Dirichlet BCs on different parts of its boundary. On the Earth's surface we use the gravity disturbances generated from the DNSC08 altimetry-derived data, the EGM2008 geopotential model or from original gravity data in the regional experiment. They represent the oblique derivative BC that are projected into the Neumann BC. On the artificial upper and side boundaries we consider the Dirichlet BC generated from ITG-GRACE03S satellite model.

Consequently, in comparison with the previous approaches, not only the disturbing potential on the Earth's surface was an objective of computations but the full 3D solution was obtained directly. Our numerical method was developed for spherical domains and also for the part of boundary given by the real Earth's surface discretized by series of triangles. Method was successfully applied in different parts of the world, using different levels of discretization in order to determine the quasigeoidal heights. Our solutions were compared with EGM2008 based on spherical harmonics and in area of Slovakia verified by GPS/levelling test. It is worth noting that the gained local solutions of continental scale are in a good agreement with EGM2008. The precision of the regional quasigeoid model obtained by FEM in the area of Slovakia when using the original gravity data is comparable with solutions computed by the FFT-based methods. The results are promising for further investigation.

References

Andersen OB, Knudsen P, Berry P (2008) The DNSC08 ocean wide altimetry derived gravity field. Presented at EGU-2008, Vienna, Austria

Backus GE (1968) Application of a non-linear problem boundary-value problem for Laplace's equation to gravity and geomagnetic intensity surveys. Q J Mech Appl Math 2:195–221

Bjerhammar A, Svensson L (1983) On the geodetic boundary-value problem for a fixed boundary surface-satellite approach. Bull Géod 57:382–393

Brenner SC, Scott LR (2002) The mathematical theory of finite element methods. 2. Springer-Verlag, New York

Čunderlík R (2004) The boundary element method applied to the Neumann geodetic boundary value problem. PhD. Thesis. SvF STU, Bratislava

Čunderlík R, Mikula K (2008) On high-resolution global gravity field modelling by direct BEM using DNSC08. In: Gravity, geoid and earth observation, IAG Symposia, vol 134. Springer (accepted in December, in press)

Čunderlík R, Mikula K, Mojzeš M (2000) The boundary element method applied to the determination of the global quasigeoid. Proceedings of ALGORITMY, pp 301–308

Čunderlík R, Mikula K, Mojzeš M (2008) Numerical solution of the linearized fixed gravimetric boundary-value problem. J Geod 82(1):15–29

Grafarend EW (1989) The goid and the gravimetric boundary-value problem. Rep. 18, Department of Geod, The Royal Institute of Technology, Stockholm

Holota P (1997) Coerciveness of the linear gravimetric boundary-value problem and a geometrical interpretation. J Geod 71(10):640–651

Holota P (2005) Neumann's boundary-value problem in studies on Earth gravity field: weak solution. 50 years of Research Institute of Geodesy, Topography and Cartography, Prague, vol 50, pp 34, 49–69

Holota P, Nesvadba O (2008) Model refinements and numerical solutions of weakly formulated boundary-value problems in physical geodesy. In: Proceedings of VI Hotine-Marussi symposium on theoretical and computational geodesy. Springer, Berlin

Klees R (1992) Loesung des fixen geodaetischen Randwertprolems mit Hilfe der Randelementmethode. DGK. Reihe C., Nr. 382, Muenchen

Klees R (1995) Boundary value problems and approximation of integral equations by finite elements. Manuscr Geod 20:345–361

Klees R (1998) Topics on boundary element methods. Geodetic boundary value problems in view of the one centimeter geoid. Lecture Notes in Earth Sciences, vol 65. Springer, Heidelberg 482–531

Klees R, Van Gelderen M, Lage C, Schwab C (2001) Fast numerical solution of the linearized Molodensky prolem. J Geod 75:349–362

Klobušiak M, Pecár J (2004) Model and algorithm of effective processing of gravity measurements performed with a group of absolute and relative gravimeters. GaKO 50/92, No. 4–5, pp 99–110

Koch KR, Pope AJ (1972) Uniqueness and existence for the geodetic boundary value problem using the known surface of the earth. Bull Géod 46:467–476

Lehmann R (1977) Fast space-domain evaluation of geodetic surface integrals. J Geod 71:533–540

Lehmann R (1997) Solving geodetic boundary value problems with parallel computers. Geodetic boundary value problems in view of the one centimeter Geoid. Lecture Notes in Earth Sciences, vol 65. Springer, Berlin

Lehmann R, Klees R (1996) Parallel setup of Galerkin equation system for a geodetic boundary value problem. Boundary elements: implementation and analysis of advanced algorithms. Notes on Numerical Fluid Mehanics 54. Vieweg Verlag, Braunschweig

Mayer-Grr T (2007) ITG-Grace03s: The latest GRACE gravity field solution computed in Bonn. Presentation at GSTM+SPP, 15–17 October, Potsdam

Meissl P (1981) The use of finite elements in physical geodesy. Report 313, Geodetic Science and Surveying, The Ohio State University

Mojzeš M, Janák J, Papčo J (2006) Improvement of the gravimetric model of quasigeoid in Slovakia. Newton's Bulletin 3. http://bgi.cnes.fr:8110/Mojzes.pdf

Molodenskij MS, Jeremejev BF, Jurkina MI (1962) Methods for study of the external gravitational field and figure of the Earth. Israel program for scientific translations, Jerusalem (translated from Russian original, Moscow 1960)

Moritz H (1980) Advanced physical geodesy. Helbert Wichmann Verlag, Karlsruhe

Nesvadba O, Holota P, Klees R (2007) A direct method and its numerical interpretation in the determination of the Earth's gravity field from terrestrial data. In: Tregoning P, Rizos C (eds) Dynamic planet–monitoring and understanding a dynamic planet with geodetic and oceanographic tools. IAG Symposium, Cairns, Australia, 22–26, August 2005, chap. 54, vol 130. Springer, Berlin, pp 370–376

Pavlis NK, Holmes SA, Kenyon SC, Factor JK (2008) An Earth grav-itational model to degree 2160: EGM2008, presented at the 2008 General Assembly of EGU, Vienna, Austria

Reddy JN (1993) An introduction to the finite element method. 2. Mc Graw-Hill, Singapore

Rektorys K (1974) Variační metody v inženýrských problémech a v problémech matematické fyziky. STNL, Praha (in Czech)

Sacerdote F, Sansó F (1989) On the analysis of the fixed-gravimetric boundary value problem. In: Proceedings of the 2nd Hotine-Maris-ssi Symp. Math. Geod, Pisa, Politecnico di Milano, pp 507–516

Shaofeng B, Dingbo C (1991) The finite element method for the geo-detic boundary value problem. Manuscr Geod 16:353–359

Sideris MG, Schwarz KP (1986) Solving Molodensky's series by fast Fourier transform techniques. Bull Geod 60:51–63

Šprlák M, Janák J (2006) Gravity field modeling. New program for gravity field modeling by spherical harmonic functions. GaKO 1:1–8

Stokes GG (1849) On the variation of gravity at the surface of the Earth. Trans Cambridge Philos Soc 8(5):672–695

Tscherning CC (1978) Collocation and least squares methods as a tool for handling gravity field dependent data obtained through space research techniques. In: Hieber S, Guyenne TD (eds) On space oceanography, navigation and geodynamics European workshop. European Space Agency, pp 141–149

Vaníček P, Krakiwsky E (1982) Geodesy—the concepts. The North-Holland Publishing Company, Amsterdam